JOC The Journal of Organic Chemistry

Note

pubs.acs.org/joc

SET-Induced Biaryl Cross-Coupling: An $S_{RN}1$ Reaction

Brandon E. Haines[†] and Olaf Wiest*[,†,‡]

[†]Department of Chemistry and Biochemistry, University of Notre Dame, Notre Dame, Indiana 46556, United States

[‡]Laboratory of Computational Chemistry and Drug Design, Laboratory of Chemical Genomics, Peking University Shenzhen Graduate School, Shenzhen 518055, China

Supporting Information

ABSTRACT: The SET-induced biaryl cross-coupling reaction is established as the first example of a Grignard $S_{RN}1$ reaction. The reaction is examined within the mechanistic framework of dissociative electron transfer in the presence of a Lewis acid. DFT calculations show that the reaction proceeds through a radical intermediate in the form of an Mg ion-radical cage, which eludes detection in trapping experiments by reacting quickly to form an $MgPh_2$ radical anion intermediate. A new mechanism is proposed.

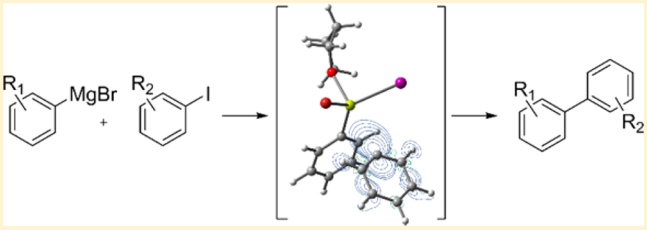

The cross-coupling of aryl metal reagents with aryl halides is a widely used method for the synthesis of biaryl compounds, which are of great interest in the preparation of bioactive molecules, natural products, and polymers.[1−5] This reaction is most commonly performed by transition-metal catalysis, but there is significant interest in transition-metal-free cross-coupling reactions due to advantages in ease of purification as well as lower toxicity and cost.[6−9] While various advances in the transition-metal-free synthesis of biaryls have thus been reported,[10−13] Hayashi and co-workers have demonstrated an important example by coupling easily accessible aryl magnesium bromides with aryl iodides and bromides as illustrated in Scheme 1.[14]

Scheme 1. Reaction Conditions for the SET-Induced Biaryl Cross-Coupling Reaction[14]

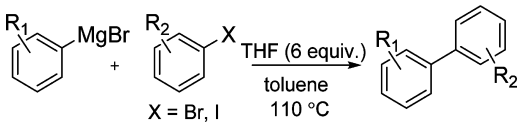

The mechanism of this reaction is unclear. Based on the reactivity differences between aryl bromides and iodides,[14] the reaction was originally classified as a nucleophilic radical chain ($S_{RN}1$) reaction where the aryl halide (ArX) is activated via single-electron transfer (SET). However, there is little precedent for an organometallic reagent acting as the nucleophile in an $S_{RN}1$ reaction.[15]

Further questions about the mechanism of the reaction arose based on a radical clock reaction using 2-(3-butenyl)phenyl iodide ($k_{cyclization} = 5 \times 10^8\ s^{-1}$ at 50 °C).[16] The coupling product was formed in 90% yield with essentially none of the radical-trapping products.[17] Hayashi and co-workers have also reported a coupling reaction between arylmagnesium bromides and alkenyl halides that is suggested to occur via the same mechanism. In this reaction, retention of the stereochemistry of the double bond is observed.[18] These results were interpreted as evidence that the reaction proceeds without the formation of a radical intermediate. This mechanism, shown in Scheme 2,

Scheme 2. Proposed Mechanism for the SET-Induced Biaryl Cross-Coupling Reaction[17]

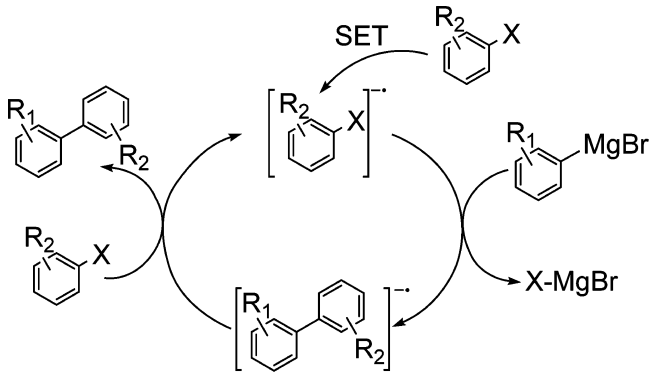

postulates a direct coupling of $ArX^{\bullet-}$ and ArMgBr. Such an $S_{RN}2$ mechanism has been discussed extensively in the literature and is unlikely due to charge repulsion, orbital arguments, or expected radical anion lifetime.[19−21] In agreement with these previous findings, we were unable to locate stationary points associated with an $S_{RN}2$ mechanism during the studies described here. Instead, all optimizations led to a dissociation of the carbon−iodide bond and the structures described below.

Given these unresolved questions and the high level of interest in the reaction, we undertook a computational study and propose a new mechanism that is consistent with the

Received: January 28, 2014
Published: February 24, 2014

   dx.doi.org/10.1021/jo500222d | J. Org. Chem. 2014, 79, 2771−2774

available experimental results. We started our investigation by considering the interaction of the THF-complexed Grignard reagent with the phenyl iodide radical anion.[22] It was shown previously that aryl halides generally have sufficiently low energy π^* orbitals to form a stable π-radical anion (π-RA) species upon accepting an electron.[23−25] A calculation of the activated complex for the analysis of the electronic structure of the resulting phenyl iodide π-RA shows that the SOMO has nodes at the *ipso*- and *para*-carbons relative to the halide,[26] indicating that no interactions can take place at these positions. The lowest energy structures, **o-1** and **m-1**, with the Mg atom localized at the *ortho*- and *meta*-positions of the phenyl iodide π-RA, respectively, are shown in Figure 1 (see Figure S1 in the Supporting Information for a full conformational analysis). The C2−Mg bond is almost fully formed, while the C1−I bond is only slightly elongated. The *meta* isomer is 0.9 kcal/mol lower in energy than the *ortho* isomer, indicating that both species will be present in solution. It is expected that the Mg-complexed π-RA forms instantaneously upon electron transfer, as the Mg atom has a similar stabilizing effect on the π-RA as would a polar solvent.[27] The next step, halide dissociation, will result in the transfer of the iodide to the magnesium. This suggests that the reaction will proceed via the *ortho* isomer, which has the Mg and I atoms in much closer proximity.

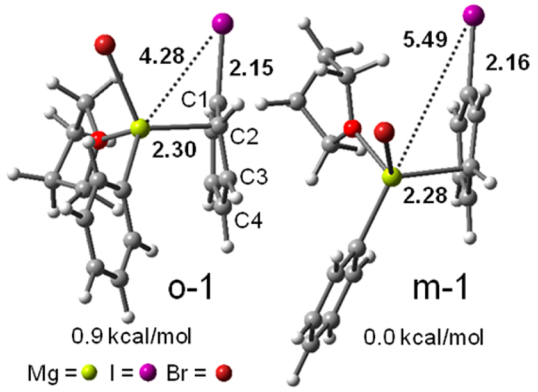

Figure 1. *Ortho* (left) and *meta* (right) isomers of the Mg complexed to the π-radical anion of aryl iodide. Distances are reported in angstroms.

The reaction coordinate for halide dissociation is complex and consists of the migration of multiple atoms and a reorientation of the aryl rings. Figure 2 shows the potential energy surface for this step as projected onto the C−X bond distance coordinate (C1−I for the phenyl iodide π-RA). The transition structure (TS) **2** with a C1−I distance of 2.17 Å was located and indicates a barrier of 2.2 kcal/mol. As is characteristic for halide dissociation from a π-RA species, the TS is bent with a C4−C1−I angle of 167.6°.[28−35] At the TS, the unpaired electron transfers from the π^* orbital of the aromatic system to the antibonding σ^* orbital of the C−X bond in a process called an intramolecular electron transfer (IET). Mixing of these orbitals is forbidden by orbital symmetry in the planar molecule, so bending of the halogen out of the plane of the π system allows the orbitals to mix, avoids an impending conical intersection, and lowers the barrier to dissociation. Structures where the halide is bent out of plane are referred here as the $\pi-\sigma$ coupling state.[26]

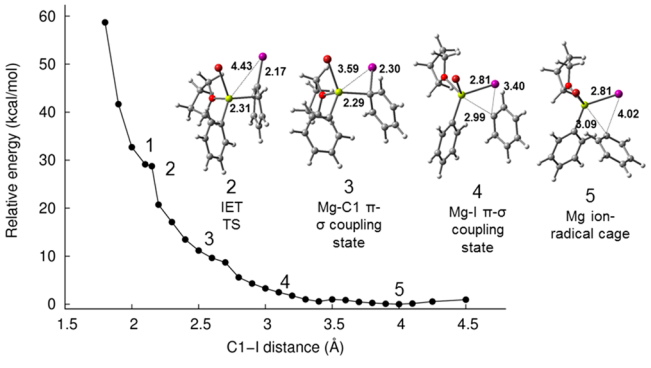

Figure 2. Potential energy surface for halide dissociation, projected onto the C1−I distance coordinate of the phenyl iodide π-RA.

After the IET transition state, with a C1−I distance of ∼2.20 Å and consistent with the σ^* character of the SOMO in the $\pi-\sigma$ coupling state, the Mg transfers to C1. This region is represented by the $\pi-\sigma$ coupling structure **3** with Mg coordinated to C1. Then, the C1−I bond elongates to ∼2.80 Å and the iodide migrates toward the Mg as represented by the $\pi-\sigma$ coupling structure **4**, which, due to remaining orbital interactions with the iodine, positions the aryl group perpendicular to the Grignard aryl group. To form the new carbon−carbon bond, the aryl group has to dissociate from the iodine and rotate to be parallel to the Grignard aryl group. In Figure 2, this step is indicated by the bump at ∼3.50 Å.

The final step is the formation of the Mg ion-radical cage **5** where the C−I bond is fully broken (C1−I = 4.02 Å). In this structure, the SOMO is located almost entirely on the halide aryl group. This indicates that the aryl radical, in contrast to the previous mechanistic proposal,[17] is an intermediate in this reaction. Typically, a minimum of this type is associated with a loose, planar complex in which the SOMO is located fully in the σ^* orbital of the C−X bond, also known as the σ radical anion (σ-RA). The formation and stability of the σ-RA intermediate is also dependent on potential interaction partners, such as solvent molecules.[36,37] For example, more polar solvents decrease the stability of the σ-RA by solvating the anionic leaving group. The Mg atom appears to play a similar role by stabilizing the I^- leaving group and preventing the formation of a σ-RA intermediate.

The radical character of the aryl group suggested in structure **5** is in apparent contradiction to the results of the radical clock experiments. This discrepancy can be resolved on the basis of the hypothesis that the aryl radical reacts faster toward the product than it reacts in the radical clock reaction. To study this possibility, we scanned the distance between the aryl radical and the Mg atom (see Figure S2 in the Supporting Information) and located a transition structure **6** at a C1−Mg distance of 2.72 Å. The calculated barrier of 1.0 kcal/mol is significantly lower than the experimentally determined activation energy for the radical clock cyclization reaction of approximately 3.5 kcal/mol at 50 °C.[16] The experimentally observed lack of cyclization product is therefore in agreement with the computational results.

In addition to the lower barrier, the analysis of the electronic structure of the product **7** (see the spin plots in Figure S3 of the Supporting Information) shows that the radical is delocalized across both aryl groups to form a $MgBrIPh_2$ radical anion. This delocalization process lowers the spin density and should make trapping of the radical difficult as there are few radical clock reactions fast enough to compete with it. Conversely, the complete dissociation of the aryl radical away from the Mg ion

dx.doi.org/10.1021/jo500222d | J. Org. Chem. 2014, 79, 2771−2774

cage to engage in side reactions is also unlikely to occur as the dissociated product is at least 6 kcal/mol uphill.[38]

There are two possible pathways for the conversion of the $MgBrIPh_2$ radical anion to the aryl coupling product. To study the pathway where ET occurs after the coupling reaction, the distance between C1 and C1′ was scanned, and a transition structure **8** was located at a C1−C1′ distance of 2.19 Å as shown in Figure 3.[39] The product biaryl radical anion **9** is

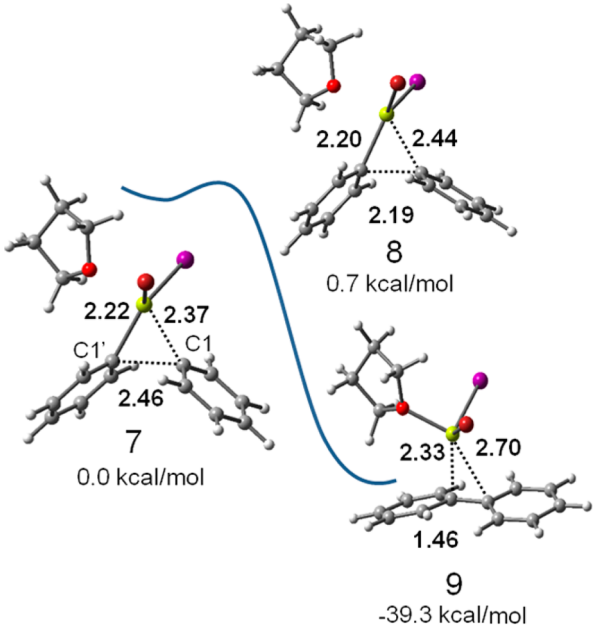

Figure 3. Reaction sequence for the formation of the biaryl radical anion through the $MgBrIPh_2$ radical anion.

complexed with MgBrI, and the barrier is predicted to be 0.7 kcal/mol. In the alternative pathway, where the ET occurs from the $MgBrIPh_2$ radical anion, the complex is calculated to form the coupling product and MgBrI without barrier after removal of an electron. This result is consistent with the idea that the extra electron holds the $MgBrIPh_2$ radical anion complex together. These results are also consistent with the experimentally observed stereochemical outcome of the reaction with alkenyl halides. While a free alkenyl radical would scramble the stereochemistry of the double bond, the interaction of the alkenyl radical with the Mg atom renders the isomerization process slower than the coupling reaction.[18] Similar to the results for the radical clock experiments, the experimentally observed selectivity is therefore a result of the very fast coupling reaction rather than an indication that no radical is present.

These calculations strongly suggest that the reaction proceeds through a radical intermediate which quickly reacts to form a $MgBrIPh_2$ radical anion. The mechanism that emerges from these results is shown in Scheme 3. It can be classified as a novel variation of the $S_{RN}1$ reaction where the radical intermediate reacts very quickly and nucleophilic combination is facilitated by magnesium. The reaction is calculated to be highly exothermic. This is in agreement with previous studies of Grignard reactions[40,41] and due to the replacement of the weak carbon−magnesium bond with a stable, conjugated carbon−carbon bond. The calculated barriers are low, which supports the idea that the initial SET is rate-

Scheme 3. Proposed Mechanism of the SET-Induced Biaryl Cross-Coupling Reaction

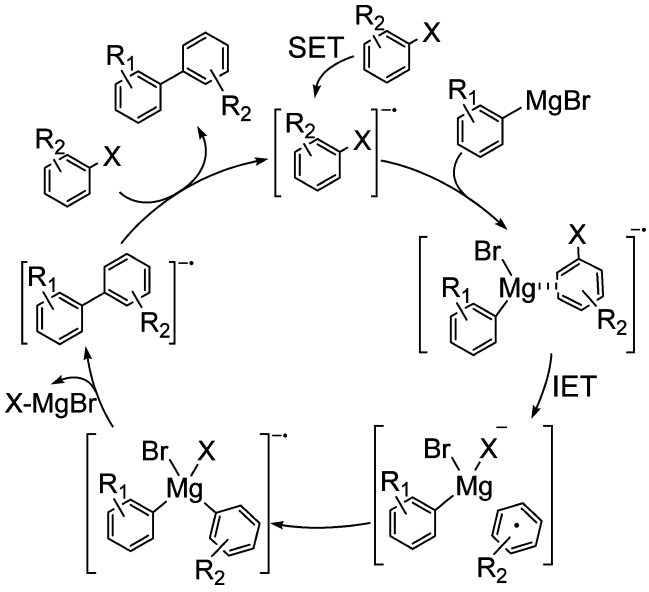

limiting and necessary for the "spontaneous initiation" element of the mechanism.[14,17]

The mechanism proposed here may also be applicable to other biaryl cross-coupling reactions involving arylmetal reagents[13,42] and could be envisioned as an $S_{RN}1$ reaction with an additional π-Lewis acid to stabilize the π-RA independent of the reacting Grignard reagent. Finally, this mechanistic understanding of the reaction can provide a starting point for the asymmetric synthesis of chiral biaryl systems, a class of compounds that has found intense interest in the past few years.[43−45]

EXPERIMENTAL SECTION

Phenylmagnesium bromide and phenyl iodide were used to model the reaction. The Grignard reagent was represented as a monomer with various degrees of THF coordination based on the hypothesis that the presence of THF breaks up higher order aggregates of the Grignard reagent.[14,17] Because the focus of this work is on the coupling mechanism and the energy of the activated complex for the electron-transfer step cannot be calculated reliably with the methods used here, the phenyl iodide radical anion was used as the starting point. It should be noted that the initiation and propagation electron-transfer steps are likely to be the rate-determining steps, accounting for the high temperatures and long reaction times necessary for the reaction.[14]

All calculations were carried out with the Gaussian 09 (G09) suite of programs.[46] Full geometry optimizations of stationary points were calculated at the M06/SDD level for Br and I and M06/6-31+g(d) for all other atoms. The integral equation formalism polarizable continuum (IEFPCM) solvation model with parameters for toluene was applied in accordance with experiment to account for solvation effects.[47−49] Single-point energies were calculated using the aug-cc-pVTZ-PP basis set[50] for I, which was obtained from the EMSL basis set library using the Basis set exchange software,[51,52] and 6-311++g(2d,2p) for all other atoms with solvation correction from the IEFPCM model. Energies reported for stationary points are Gibbs free energies calculated at 298 K and 1 atm of pressure. Frequency calculations were used to characterize the structures either as a ground state (zero negative frequencies) or as a transition state (exactly one negative frequency). Intrinsic reaction coordinate (IRC) calculations were performed for transition states to ensure they connect the correct reactant and product. In the case of the radical delocalization process, the potential energy surface (PES) around the transition state (TS) is

dx.doi.org/10.1021/jo500222d | J. Org. Chem. 2014, 79, 2771−2774

very flat so IRC calculations were unsuccessful. However, manual distortion along the imaginary mode in either direction followed by full optimization led to the correct reactant and product. For the PES in Figure 2, a series of constrained optimizations were performed, where the C1−I distance was constrained. Only the electronic energy is reported for these calculations.

■ ASSOCIATED CONTENT

Supporting Information

Details of the computational methods used, additional references and the complete ref 46, additional analysis as referred to in the text, and coordinates of the characterized stationary points are provided. This material is available free of charge via the Internet at http://pubs.acs.org.

■ AUTHOR INFORMATION

Corresponding Author

*Email: owiest@nd.edu. Tel: 574-631-5876.

Notes

The authors declare no competing financial interest.

■ ACKNOWLEDGMENTS

We thank the National Science Foundation (NSF CHE 1058075) for financial support and the Center for Research Computing at the University of Notre Dame and the TeraGrid (TG-CHE12050) for generous allocation of computational resources. We also thank Prof. Per-Ola Norrby (Astra-Zeneca and University of Gothenburg) for helpful discussions. B.E.H. is the recipient of a Graduate Fellowship from the CBBI Program at the University of Notre Dame (NIGMS Grant No. T32-075762).

■ REFERENCES

(1) Stanforth, S. P. *Tetrahedron* **1998**, *54*, 263−303.
(2) Hassan, J.; Sevignon, M.; Gozzi, C.; Schulz, E.; Lemaire, M. *Chem. Rev.* **2002**, *102*, 1359−1469.
(3) Alberico, D.; Scott, M. E.; Lautens, M. *Chem. Rev.* **2007**, *107*, 174−238.
(4) Ashenhurst, J. A. *Chem. Soc. Rev.* **2010**, *39*, 540−548.
(5) Murarka, S.; Studer, A. *Angew. Chem., Int. Ed.* **2012**, *51*, 12362−12366.
(6) Leadbeater, N. E. *Nat. Chem.* **2010**, *2*, 1007−1009.
(7) Shirakawa, E.; Hayashi, T. *Chem. Lett.* **2012**, *41*, 130−134.
(8) Mehta, V. P.; Punji, B. *RSC Adv.* **2013**, *3*, 11957−11986.
(9) Arancon, R. A. D.; Lin, C. S. K.; Vargas, C.; Lugue, R. *Org. Biomol. Chem.* **2014**, *12*, 10−35.
(10) Leroux, F. R.; Berthelot, A.; Bonnafoux, L.; Panossian, A.; Colobert, F. *Chem.—Eur. J.* **2012**, *18*, 14232−14236.
(11) Gao, H. Y.; Ess, D. H.; Yousufuddin, M.; Kurti, L. *J. Am. Chem. Soc.* **2013**, *135*, 7086−7089.
(12) Dewanji, A.; Murarka, S.; Curran, D. P.; Studer, A. *Org. Lett.* **2013**, 6102−6105.
(13) Minami, H.; Wang, X.; Wang, C.; Uchiyama, M. *Eur. J. Org. Chem.* **2013**, 7891−7894.
(14) Shirakawa, E.; Hayashi, Y.; Itoh, K.; Watabe, R.; Uchiyama, N.; Konagaya, W.; Masui, S.; Hayashi, T. *Angew. Chem., Int. Ed.* **2012**, *51*, 218−221.
(15) Rossi, R. A.; Pierini, A. B.; Penenory, A. B. *Chem. Rev.* **2003**, *103*, 71−167.
(16) Abeywickrema, A. N.; Beckwith, A. L. J. *J. Chem. Soc., Chem. Commun.* **1986**, 464−465.
(17) Uchiyama, N.; Shirakawa, E.; Hayashi, T. *Chem. Commun.* **2013**, *49*, 364−366.
(18) Shirakawa, E.; Watabe, R.; Murakami, T.; Hayashi, T. *Chem. Commun.* **2013**, *49*, 5219−5221.
(19) Denney, D. B.; Denney, D. Z. *Tetrahedron* **1991**, *47*, 6577−6600.
(20) Bunnett, J. F. *Tetrahedron* **1993**, *49*, 4477−4484.
(21) Rossi, R. A.; Palacios, S. M. *Tetrahedron* **1993**, *49*, 4485−4494.
(22) See Figure S1 in the Supporting Information for a conformational analysis of the Mg−π-RA.
(23) Andrieux, C. P.; Saveant, J. M.; Su, K. B. *J. Phys. Chem.* **1986**, *90*, 3815−3823.
(24) Steelhammer, J. C.; Wentworth, W. E. *J. Chem. Phys.* **1969**, *51*, 1802−1814.
(25) Wentworth, W. E.; Becker, R. S.; Tung, R. *J. Phys. Chem.* **1967**, *71*, 1652−1665.
(26) Pierini, A. B.; Vera, D. M. A. *J. Org. Chem.* **2003**, *68*, 9191−9199.
(27) Costentin, C.; Robert, M.; Saveant, J. M. *J. Am. Chem. Soc.* **2004**, *126*, 16834−16840.
(28) Pierini, A. B.; Duca, J. S. *J. Chem. Soc., Perkin Trans. 2* **1995**, 1821−1828.
(29) Pierini, A. B.; Duca, J. S.; Vera, D. M. A. *J. Chem. Soc., Perkin Trans. 2* **1999**, 1003−1009.
(30) Beregovaya, I. V.; Shchegoleva, L. N. *Chem. Phys. Lett.* **2001**, *348*, 501−506.
(31) Laage, D.; Burghardt, I.; Sommerfeld, T.; Hynes, J. T. *J. Phys. Chem. A* **2003**, *107*, 11271−11291.
(32) Laage, D.; Burghardt, I.; Sommerfeld, T.; Hynes, J. T. *ChemPhysChem* **2003**, *4*, 61−66.
(33) Burghardt, I.; Laage, D.; Hynes, J. T. *J. Phys. Chem. A* **2003**, *107*, 11292−11306.
(34) Takeda, N.; Poliakov, P. V.; Cook, A. R.; Miller, J. R. *J. Am. Chem. Soc.* **2004**, *126*, 4301−4309.
(35) Costentin, C.; Robert, M.; Saveant, J. M. *J. Am. Chem. Soc.* **2004**, *126*, 16051−16057.
(36) Cardinale, A.; Isse, A. A.; Gennaro, A.; Robert, M.; Saveant, J. M. *J. Am. Chem. Soc.* **2002**, *124*, 13533−13539.
(37) Costentin, C.; Robert, M.; Saveant, J. M. *Chem. Phys.* **2006**, *324*, 40−56.
(38) This energy is reported at a C1−I distance of 6.00 Å.
(39) We also considered other THF complexes. The complex with two THF molecules coordinated is not a stable structure. The complexes with one and no THF molecules are approximately equal in energy, and in both cases the coupling reaction is predicted to be very fast and energetically favorable.
(40) Yamazaki, S.; Yamabe, S. *J. Org. Chem.* **2002**, *67*, 9346−9353.
(41) Ye, J. L.; Huang, P. Q.; Lu, X. *J. Org. Chem.* **2007**, *72*, 35−42.
(42) Shirakawa, E.; Tamakuni, F.; Kusano, E.; Uchiyama, N.; Konagaya, W.; Watabe, R.; Hayashi, T. *Angew. Chem., Int. Ed.* **2014**, *53*, 521−525.
(43) Bringmann, G.; Mortimer, A. J. P.; Keller, P. A.; Gresser, M. J.; Garner, J.; Breuning, M. *Angew. Chem., Int. Ed.* **2005**, *44*, 5384−5427.
(44) Kozlowski, M. C.; Morgan, B. J.; Linton, E. C. *Chem. Soc. Rev.* **2009**, *38*, 3193−3207.
(45) Zask, A.; Murphy, J.; Ellestad, G. A. *Chirality* **2013**, *25*, 265−274.
(46) Gaussian 09, Revision C.01: Frisch, M. J. et al.. Gaussian Inc., Wallingford, CT, 2009. See the Supporting Information for the full reference.
(47) Cances, E.; Mennucci, B.; Tomasi, J. *J. Chem. Phys.* **1997**, *107*, 3032−3041.
(48) Cossi, M.; Barone, V.; Mennucci, B.; Tomasi, J. *Chem. Phys. Lett.* **1998**, *286*, 253−260.
(49) Mennucci, B.; Cances, E.; Tomasi, J. *J. Phys. Chem. B* **1997**, *101*, 10506−10517.
(50) Peterson, K. A.; Shepler, B. C.; Figgen, D.; Stoll, H. *J. Phys. Chem. A* **2006**, *110*, 13877−13883.
(51) Feller, D. *J. Comput. Chem.* **1996**, *17*, 1571−1586.
(52) Schuchardt, K. L.; Didier, B. T.; Elsethagen, T.; Sun, L. S.; Gurumoorthi, V.; Chase, J.; Li, J.; Windus, T. L. *J. Chem. Inf. Model* **2007**, *47*, 1045−1052.